Anti-tumor effects of isoliquiritigenin in Bcl-2/Bax and PCNA expression of T24 human bladder cancer cells

Zhanbin Huang[1], Qianmei Wu[2], Zhong Wang[1]

[1]The First Affiliated Hospital of Guangdong Pharmaceutical University, Yuexiu district, Guangzhou, Guangdong Province, China
[2]Guangdong Second Provincial General Hospital, Guangdong, China

Submitted: 8 August 2020
Accepted: 12 October 2020

Arch Med Sci
DOI: https://doi.org/10.5114/aoms.2020.101243

Corresponding author:
Prof. Zhong Wang
The First Affiliated Hospital
Guangdong Pharmaceutical University
19 Nonglin Xialu
Yuexiu District
Guangzhou
Guangdong Province, China
E-mail: wangzhonggdpu@163.com

Abstract

Introduction: The aim of this study was to investigate the proliferation and apoptosis of T24 after treatment with isoliquiritigenin (ISL) and to explore the underlying mechanism.

Material and methods: T24 cells were divided into 6 groups and cultured. The five experimental groups were seeded into medium with 10, 20, 40, 80, and 160 μM ISL and the control group was administered with 0.01% DMSO. The cell morphology was observed using an optical microscope. The proliferation of cells and half maximal inhibitory concentration (IC_{50}) were determined and calculated by MTS. Cell cycle and apoptosis were evaluated by flow cytometry. The migration ability of cells was detected by wound healing assay. The expression of B-cell lymphoma 2 (Bcl-2), Bcl-2-associated X protein (Bax), and proliferating cell nuclear antigen (PCNA) was determined by RT-qPCR and western blot.

Results: At 24 h after treatment with ISL, morphology revealed that cell number diminished and the cell volume shrank with increasing concentration. According to the results of MTS, ISL significantly inhibited the T24 cell proliferation in a dose- and time-dependent manner. Flow cytometry showed that ISL could block the replication of T24 cell DNA from S phase to G2, therefore promoting cell apoptosis. Wound healing assay showed that at 48 h after treatment with ISL, the migration of T24 cells was remarkably inhibited. The results of RT-qPCR and Western blot revealed that after 24 h of treatment, the expression levels of Bcl-2 and PCNA were down-regulated, and the expression level of Bax was increased in the different dose of the ISL treated group.

Conclusions: ISL possesses detrimental effects on the viability of BC cell T24 in a dose-dependent manner via blocking the cell cycle and inducing apoptosis by down-regulation of PCNA and Bcl-2 expression and up-regulation of Bax expression.

Key words: isoliquiritigenin, bladder cancer, T24 cells, proliferation, apoptosis, Bcl-2/Bax, PCNA.

Introduction

Bladder cancer (BC), as one of the top ten malignant tumors in the human body, is the most common malignant tumor of the urinary system, with the highest mortality rate among urogenital tumors in China [1]. Currently, routine treatment for BC is a combination of surgery and adjuvant chemotherapy. But chemotherapeutic drugs are toxic to both

tumor cells and normal cells, causing serious side effects and leading to various organ dysfunctions [2], with unsatisfactory efficacy as well. The B-cell lymphoma 2 (Bcl-2) gene is closely related to the occurrence of tumors [3, 4]. Bcl-2 and Bcl-2-associated X protein (Bax) are important members of the Bcl2 gene family. Bcl-2 can inhibit apoptosis, while Bax can promote apoptosis. The ratio of Bcl-2 and Bax determines susceptibility to an apoptotic or survival signal [5]. Proliferating cell nuclear antigen (PCNA) plays an important role in regulating cell transition from G1 phase to S phase in the cell cycle, and its increased concentrations in S phase and G2 phase is a prerequisite for the synthesis of DNA, thereby initiating the proliferation of cancer cells [6]. Isoliquiritigenin (ISL) is one kind of isoflavone compounds extracted from natural Chinese herbal medicines, such as licorice root. It is the main biological active component in licorice root. ISL has been widely used in treatment of tumors and their complications, because of its mild medicinal properties and limited toxic and side effects [7]. Meanwhile, its anti-inflammatory [8] and anti-tumor [9] activities have been proved *in vivo* and *in vitro*. Previous research has shown that ISL can suppress the proliferation of lung cancer cells as well as inducing cell apoptosis in G1 phase through increasing expression of p53 and p21/WAF1 proteins, which leads to cell cycle arrest [10]. It can also inhibit the proliferation, invasion and migration of gastric cancer, prostate cancer, and breast cancer cells [11–13]. More importantly, appropriate doses of ISL are non-toxic to normal cells and tissues [14], ensuring its safety in clinical. Recent studies have confirmed that ISL can significantly reduce the proliferation rate of T24 cells and increase the apoptosis rate of T24 cells in a dose-dependent manner [15]. T24 cells exhibit typical morphology of apoptosis after treatment with ISL, including nuclear shrinkage, nuclear fragmentation, chromosome edge set, etc. It is speculated that the anti-tumor mechanism of ISL might be associated with the increase of CDK2 viability, the down-regulation of inner mitochondrial membrane potential (DeltaPsim), and activation of the caspase-3/9-mediated mitochondrial apoptotic signaling pathway [15–18], but the specific molecular mechanism of ISL in cancer treatment remains unclear.

In this study, we aimed to investigate the inhibitory effect of ISL on bladder cancer, and its effects on the expression of Bcl-2/Bax and PCNA in BC T24 cells.

Material and methods

Materials and instruments

T24 human bladder cancer cells (Institute of Biochemistry and Cell Biology, CAS); isoliquiritigenin (961-29-5 standard product, Shanghai Guangrui Biotechnology Co., Ltd); RPMI-1640 (Hyclone, Cat. No. SH30809.01B) and fetal bovine serum (FBS) (Hyclone, Cat. No. SH30087.01); penicillin and streptomycin (Hyclone, Cat. No. SH30010); phosphate buffer saline (PBS) (Hyclone, Cat. No. SH30256.01B), Annexin V-FITC apoptosis detection kit (keygen, Cat.No.KGA106); cell cycle detection kit (keygen, Cat.No.KGA511).

Suzhou Antai clean bench (SW-CJ-IFD); low speed centrifuge (Zhongjia, SC3614); inverted optical microscope (OLYMPUS CKX41, U-CTR30-2); cell incubator (Thermo scientific, HERACELL150i).

Cell culture and grouping

T24 cells were cultured in the RPMI-1640 medium supplemented with 10% FBS, 100 IU/ml penicillin and 10 mg/mL streptomycin and maintained in a humidified atmosphere containing 5% CO_2 at 37°C. The cultured T24 cells were divided into six groups: a control group and five groups treated with 10 µM, 20 µM, 40 µM, 80 µM, 160 µM ISL respectively. At 24 h after treatment with ISL with different concentrations, the morphological changes of T24 cells were observed under an inverted optical microscope and photographed.

MTS assay

According to the description of Malich [18], the cells were seeded into a 96-well culture plate. After cell adhesion, the cells were collected at indicated time points and CellTiter 96 AQ was added at a ratio of 1 : 10. OD490 was measured by a microplate reader with MTS after 4 h of incubation. Proliferation rate = (average OD value at other time points/0-hour average OD value – 1) × 100% (same sample); inhibition rate = (1 – average OD value of experimental groups/average OD value of control group) × 100% (same time). The graphic method was used to calculate the IC50 value at 24 h, 48 h, and 72 h.

Flow cytometry to detect apoptosis

The culture medium of each group in the culture plates was transferred to 15 ml conical tubes in an ice bath. The cells were rinsed with 2 ml of PBS. Subsequently, the cells were trypsinized by 0.5 ml of trypsin (excluding EDTA) and continued to incubate as well as resuspended in pre-chilled medium in an ice bath. A total of 0.5 ml of cell suspension was transferred to a clean centrifuge tube, then 1.25 µl Annexin V-FITC was added. The cell suspension reacted at room temperature for 15 min in the dark. After that, it was centrifuged at 1000 × g for 5 min. The supernatant was aspirated before PBS was used to resuspend the

cells. After addition of 10 µl of propidium iodide (PI), apoptosis was immediately measured using a flow cytometer.

Flow cytometry to detect cell cycle

After 48 h of cell transfection, the cells of each group were collected and were washed twice with pre-chilled PBS. Seventy percent pre-chilled ethanol was added to the medium to fix the cells at 4°C overnight. Subsequently, they were centrifuged and collected and then rinsed with PBS. The cells were later suspended in 500 µl of PBS with 50 µg/ml of PI, 100 µg/ml of RNase A and 0.2% Triton X-100. Finally, they were incubated at 4°C in the dark for 30 min. Cell cycle was detected using the flow cytometer. The results were analyzed by ModFit software.

Wound healing assay

Under aseptic condition, fibronectin was added to a 6-well plate at 4°C overnight. The next day, RPMI-1640 culture solution containing 10% FBS was added, and the plate was sterilized under UV for 2 h. The cell suspension in the logarithmic growth phase was uniformly seeded into the 6-well culture plate, and cultured in an incubator at 37°C with 5% CO_2. After the cells grew into a monolayer, each group was treated with mitomycin for 1 h, and the medium was replaced. Subsequently, the cell plate was scratched and the cells were rinsed 2–3 times with PBS and serum-free medium was added. The control group was cultured with serum-free RMPI-1640 medium, while the experimental groups were intervened with serum-free RMPI-1640 medium containing ISL. The samples were taken for observation at 0, 12, 24, and 48 h after culture. Image Pro-Plus 6.0 software was applied to measure the width of the scratch wounds at any eight locations of cells in each group at the same time to calculate cell migration distance and mobility.

Quantitative reverse transcription PCR (RT-qPCR) assay

The total RNA was extracted using Trizol (Invitrogen, CA, USA) according to the manufacturer's instructions, and was reversed-transcribed to cDNA as described by Li *et al*. [19]. The RT-qPCR reaction was performed under the following reaction conditions: 95°C for 5 min, 95°C for 15 s, 60°C for 30 s, 40 cycles. The *Ct* method ($2^{-\Delta\Delta Ct}$) was used for relative quantitative analysis.

Western blotting

The total protein of each group of cells was extracted by RIPA lysis buffer. After the protein concentration was measured using a BCA protein assay kit, the extracted protein solution and sample buffer were mixed in a ratio of 2 : 1 and boiled for 5 min. After 80 V constant pressure treatment for 5 min, 120 V constant voltage electrophoresis was performed until the bromophenol blue appeared on the bottom of the gel.

The hybrid membrane was rinsed with TBST for 5 min 3 times and blocked with 5% dried skimmed milk powder at room temperature for 1 h following washing. The membrane was incubated overnight at 4°C with appropriate primary antibodies (dilution rate 1 : 1000) (Anti-PCNA antibody, Cat. No.ab29; BCL-2, Cat.No.ab32124; Anti-Bax antibody, Cat.No.32503. Purchased from Abcam Co., Ltd). After rinsing with TBST for 2 min 3 times, the membrane was then incubated at 37°C for 1 h with the secondary antibodies: Rabbit Anti-Mouse IgG, Cat.No.6170-05 (Southern Biotech, 1 : 4000); Goat Anti-Rabbit IgG, Cat.No.4050-05 (Southern Biotech, 1 : 5000); Peroxidase-labeled rabbit anti-goat IgG, Cat.No.BA1060 (Wuhan Boster Biological Technology Co., Ltd, 1 : 3000); Peroxidase-labeled rabbit anti-rat IgG, Cat. No. BA1058 (Wuhan Boster Biological Technology Co., Ltd, 1 : 2000). After being rinsed with TBST, the membrane was rinsed with distilled water for 2 min 3 times. The chemiluminescent substrates were uniformly added to the surface of the membrane through a pipette and reacted for 5 min. The excess substrate solution on the surface of the membrane was absorbed with the filter paper in the kit, and then the cells were sent for development.

Statistical analysis

Data were presented as the mean ± standard deviation (SD) and were analyzed using SPSS software (version 21.0). Comparisons among multiple groups were performed using variance analysis, while comparisons between groups were performed using the Student-Newman-Keuls (SNK) method. $P < 0.05$ indicated significance.

Results

Morphology of T24 cells after ISL treatment

The morphology of the T24 cells varied after being treated with different concentrations of ISL for 24 h. In the control group, there was a large number of cells in high density, with spindle or irregular shape and strong refraction. Compared with the control group, the number and density of cells were slightly reduced in the 10 µM and 20 µM ISL treated groups. As for the 40 µM, 80 µM, and 160 µM ISL treated groups, the number of cells was gradually decreased, the cell volume was minimized and deformed, with the presence of shrinkage, roundness and shedding, and

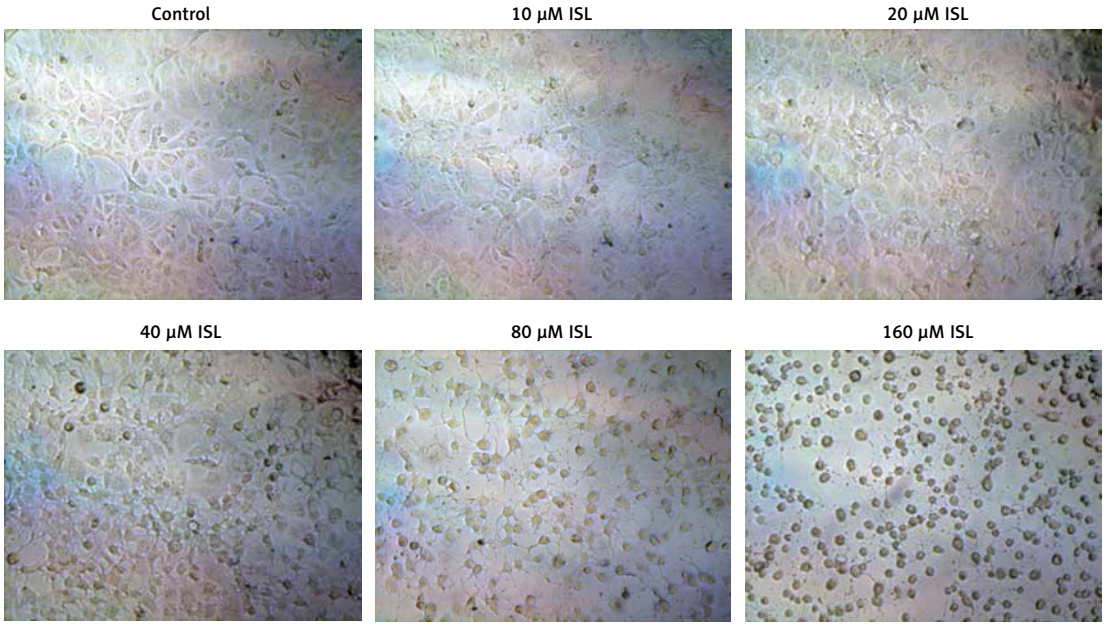

Figure 1. Morphological changes of T24 cells after treatment with different concentrations of ISL (10×). T24 cells were treated with ISL at concentrations of 10, 20, 40, 80, and 160 μM for 24 h, and morphological changes were observed under an inverted microscope

ISL – isoliquiritigenin.

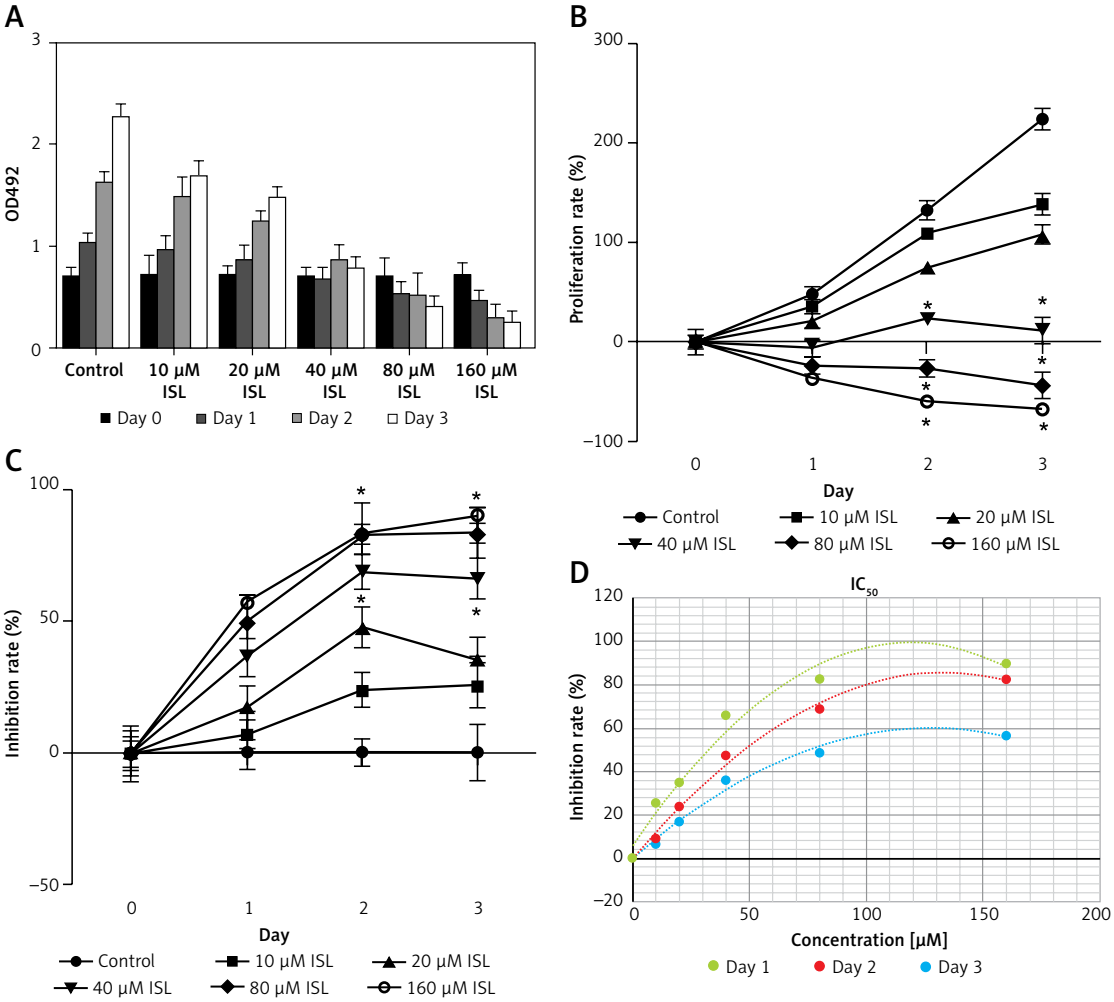

Figure 2. ISL inhibits proliferation of T24 cells. **A** – T24 cell viability was determined by MTS assay, treating with varying concentrations of ISL (10, 20, 40, 80, and 160 μM) for 24, 48, and 72 h. **B**, **C** – The proliferation rate (**B**) and inhibition rate (**C**) were calculated. **D** – IC_{50} of ISL on T24 cells at 24, 48, and 72 h

**P < 0.05 vs. control group. IC_{50} – half maximal inhibitory concentration.*

the cell refractivity was also significantly reduced (Figure 1).

ISL inhibits proliferation of T24 cells

At 24, 48, 72 h after the treatment with ISL at different concentrations, the proliferation of T24 cells was detected by MTS. Compared with the control group, the cell viability (Figure 2 A) and the proliferation rate (Figure 2 B) were decreased in the ISL treated groups in a dose-dependent manner, while the inhibition rate (Figure 2 C) showed an upward trend. Similarly, cell viability and proliferation rate also showed a downward trend and the inhibition rate of T24 cell showed an upward trend in a time-dependent manner. As shown in the IC_{50} curve regression results (Figure 2 D), it can be observed that IC_{50} = 82.34 μM on the first day, IC_{50} = 48.82 μM on the second day, and IC_{50} = 32.91 μM on the third day. These results indicated that ISL significantly inhibited T24 cell proliferation in a time- and dose-dependent manner.

ISL inhibits cell cycle of T24 cells

After treatment with ISL for 24 h, there was a reduction of cells in S phase and an accumulation of cells in G1 phase in a dose-dependent manner. Reduction of cells in G2 phase could be observed with a 160 μM dose, while the changes were not significant under a 80 μM dose. These results indicated that ISL arrested cell cycle progression from G1 to S phase (Figures 3 A, B).

ISL promotes apoptosis of T24 cells

The results of flow cytometry (Figures 4 A, B) showed that the T24 cell apoptosis was increased in the ISL treated groups in a dose-dependent manner. Compared with the control group, the apoptosis rate was significantly increased in the 40 μM, 80 μM and 160 μM ISL treated groups ($p < 0.05$). These results indicated that ISL promoted apoptosis of T24 cells *in vitro* in a dose-dependent manner.

ISL reduces migration of T24 cells

In the wound healing assay, the T24 cells were taken for observation at 0 h and 48 h after culture (Figure 5). The cells in the control group had basically fused after 48 h. With increasing concentration of ISL, the cell confluency rate became significantly slower. The cell migration rate was sig-

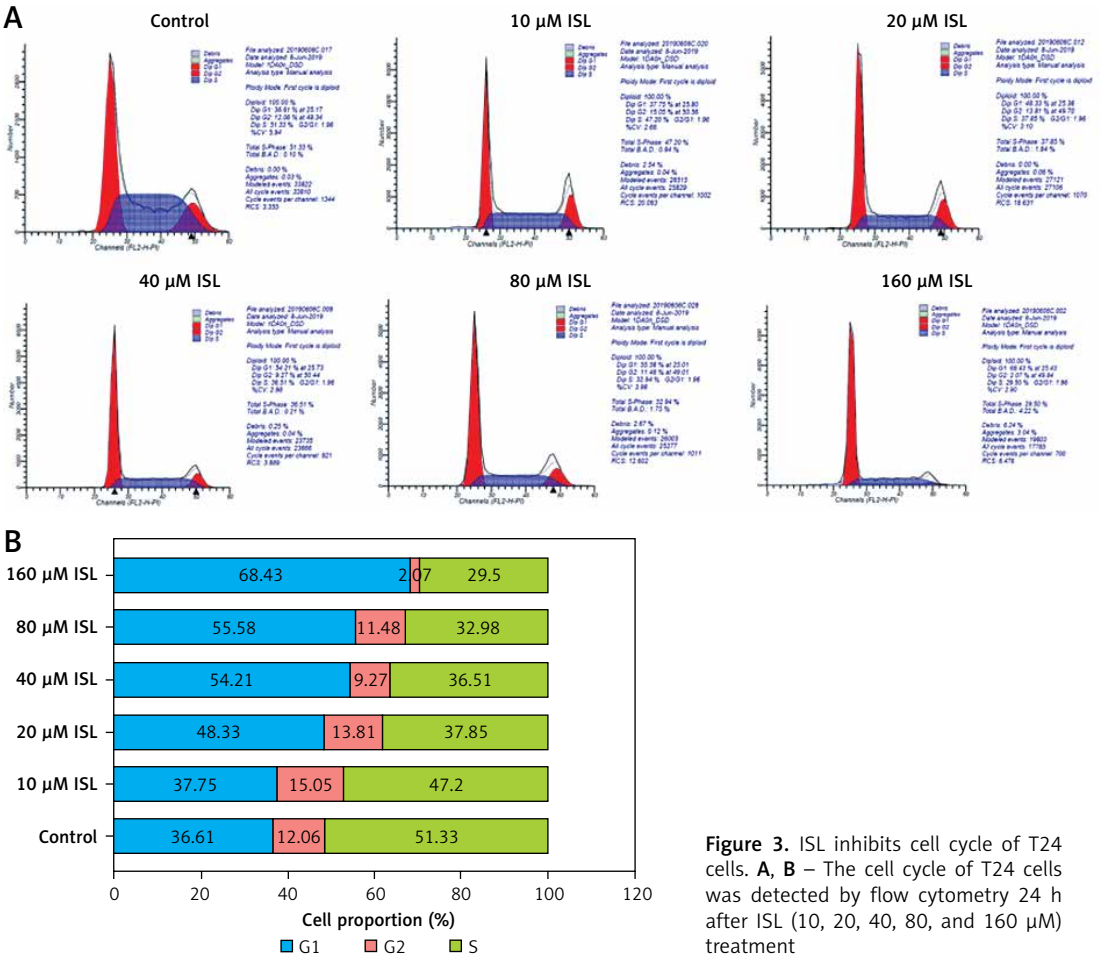

Figure 3. ISL inhibits cell cycle of T24 cells. **A**, **B** – The cell cycle of T24 cells was detected by flow cytometry 24 h after ISL (10, 20, 40, 80, and 160 μM) treatment

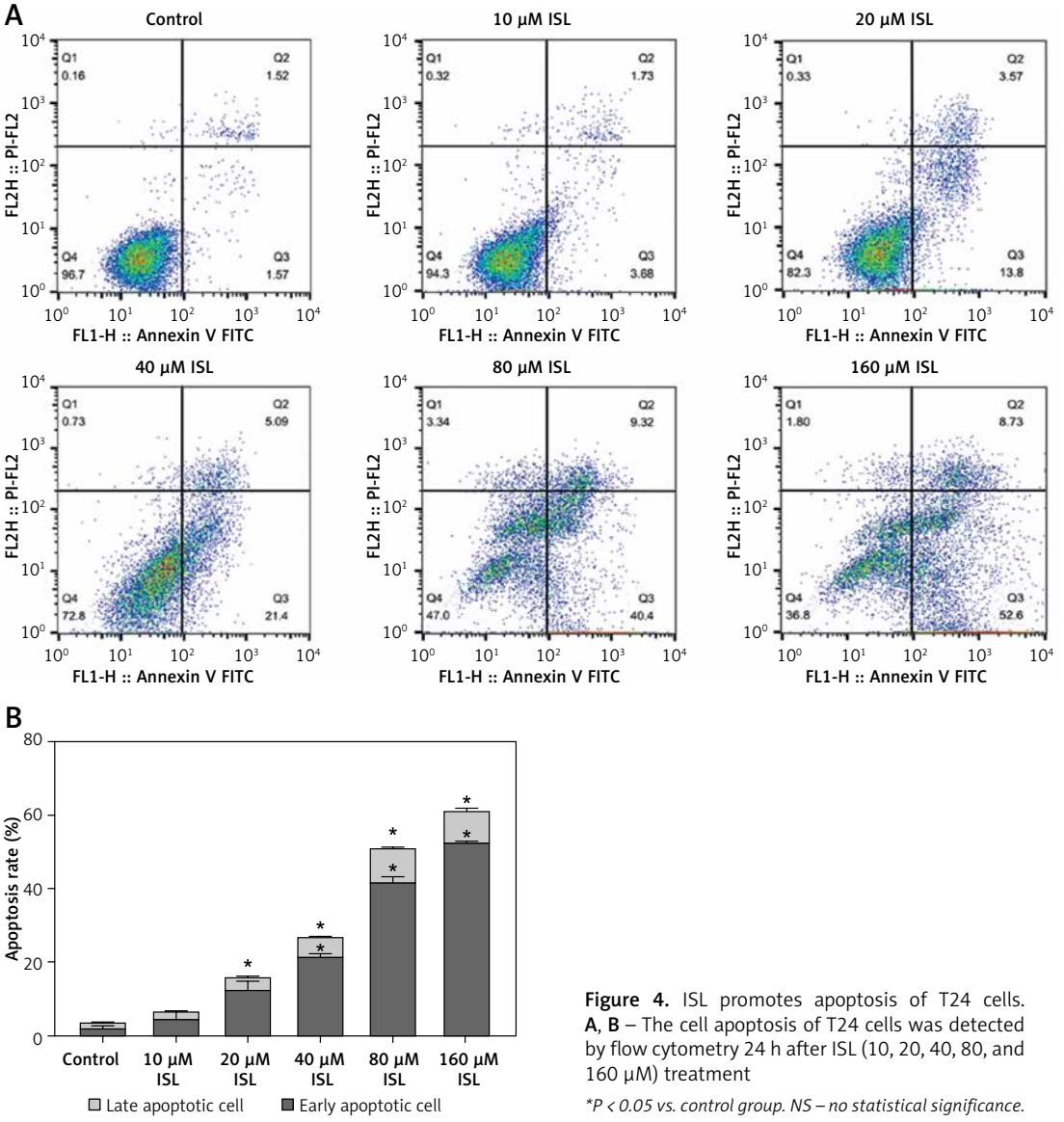

Figure 4. ISL promotes apoptosis of T24 cells. **A**, **B** – The cell apoptosis of T24 cells was detected by flow cytometry 24 h after ISL (10, 20, 40, 80, and 160 μM) treatment

**P < 0.05 vs. control group. NS – no statistical significance.*

nificantly decreased in the 80 μM and 160 μM ISL treated groups, compared with the control group.

mRNA expression of PCNA, Bcl-2, and Bax

The RT-qPCR results of PCNA, Bcl-2 and Bax after treatment with ISL for 24 h are shown in Figure 6. Compared with the control group, the mRNA expression of Bcl-2 and PCNA was decreased ($p < 0.05$) while the mRNA expression of Bax was increased gradually with increasing concentrations of ISL ($p < 0.05$).

Expression of PCNA, Bcl-2, and Bax proteins

Western blot assay was used to determine the PCNA, Bcl-2, and Bax protein expression levels in T24 cells after treatment with ISL for 24 h (Figures 7 A, B). The results showed that ISL significantly decreased PCNA and Bcl-2 protein expression and increased Bax protein expression in the T24 cells compared with the control group ($p < 0.05$).

Discussions

BC is one of the malignant tumors affecting human life with high morbidity and incidence rates, imposing a heavy social and economic burden [20–22]. The current mainstream therapy of BC has major toxic and side effects, and the problems are still unresolved. Recently, some natural herbal medicine extracts which possess limited toxic and side effects have been found to achieve a good therapeutic effect in cancer treatment, so they have become a focus in recent research. ISL is one of the most important isoflavone compounds which is isolated from licorice root and other plants. Zhou *et al.* [23] confirmed that ISL could inhibit human glioma cell proliferation and induced apoptosis *in vitro*. Wang *et al.* [24] found that ISL

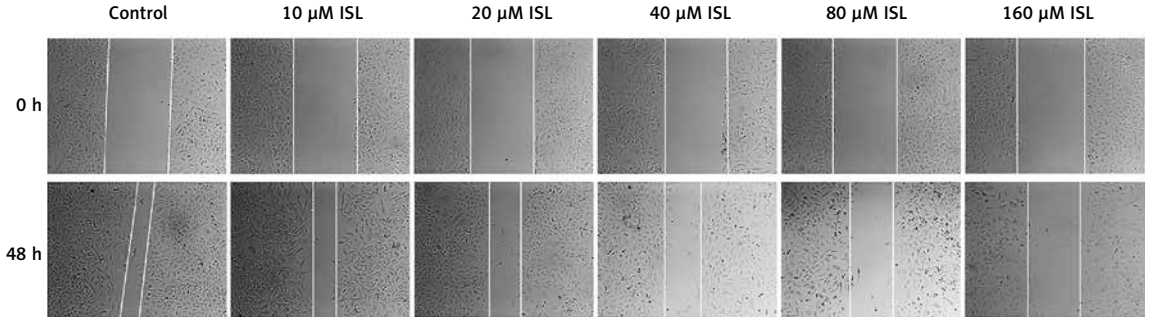

Figure 5. ISL inhibits migration of T24 cells. Wound healing assay indicated that the migration of T24 cell was decreased after ISL (10, 20, 40, 80, and 160 μM) treatment at 48 h

could inhibit the proliferation of nasopharyngeal carcinoma cells and induced apoptosis through miR-32/LATS2/Wnt. ISL also suppressed the proliferation and migration of lung cancer cells A549 [25] and osteosarcoma U2OS cells [26] through the PI3K/AKT signaling pathway. These studies have confirmed that ISL can induce apoptosis of tumor cells. In addition, the change of intracellular Bax and Bcl-2 expression ratio can affect the release of mitochondrial content, which determines the susceptibility to apoptosis [27]. ISL was proved to induce apoptosis of human cervical carcinoma HeLa cells through down-regulating the expression of Bcl-2 and Bcl-x and up-regulating Bax expression, thereby activating the apoptosis signaling pathway [28]. Based on previous research, we focused on the effect of ISL on the expression of PCNA and Bcl-2/Bax in BC T24 cells and its specific mechanism to suppress tumorigenesis.

In this study, the number of adherent T24 cells was reduced with shrinking cell volume and decreasing refractive index after treatment with ISL. In the 80 or 160 μM ISL treated groups, typical apoptotic morphology occurred, characterized as nuclear shrinkage, fragmentation, chromosome edge set, etc. In the ISL treated groups, the proliferation and migration rates of T24 cells were significantly reduced while the apoptosis was increased

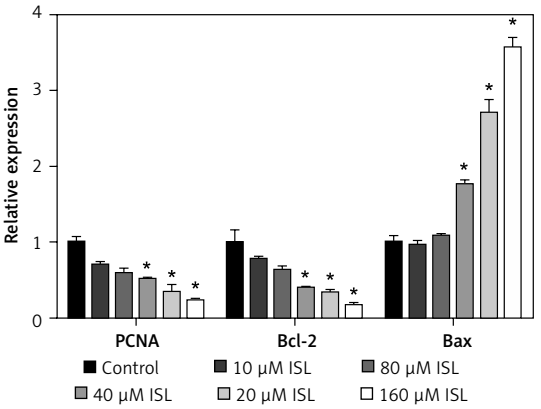

Figure 6. Effects of ISL on mRNA expression levels of PCNA, Bcl-2, and Bax in T24 cells. Expression of PCNA, Bcl-2, and Bax was detected with RT-qPCR in T24 cells treated with ISL (10, 20, 40, 80, and 160 μM) at 24 h

**P < 0.05 vs. control group.*

in a dose-dependent manner. These results demonstrate that ISL can inhibit the migration and proliferation of BC T24 cells, promote their apoptosis, and reduce their viability. According to the results of flow cytometry to detect the cell cycle, in the ISL treated groups, T24 cells at G1 phase were significantly increased in a dose-dependent manner. The early apoptosis rate added up to 52.6%

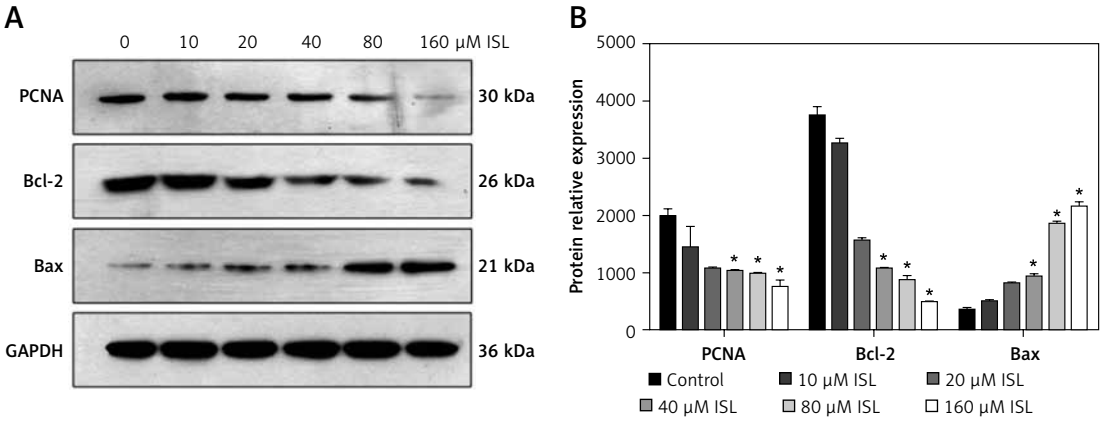

Figure 7. Protein expression of PCNA, Bcl-2, and Bax of T24 cells treated with ISL (10, 20, 40, 80, and 160 μM) for 24 h

**P < 0.05 vs. control group.*

when the dose reached 160 μM, while the G2 and S phases were significantly shortened. These results indicated that ISL arrested T24 cells at the G1 phase, hence blocking DNA replication and inhibiting the growth of T24 cells. The RT-qPCR results showed that the expression level of Bax in T24 cells increased after treatment with ISL. Notably, the expression level of Bax increased significantly in the 80 and 160 μM ISL treated groups compared with the control group, while the expression levels of Bcl-2 and PCNA increased with decreasing ISL concentration. In sum, the overall Bcl-2/Bax ratio decreased, indicating that ISL can block the process of DNA synthesis. Bax, can interact with Bcl-2 to form heterodimers or interact with itself to form homodimers. Increasing Bax homodimers often leads to apoptosis [29], while PCNA plays an important role in cell proliferation priming. Results of western blot further proved that increasing ISL concentration significantly suppressed the protein expression levels of PCNA and Bcl-2 in T24 cells and promoted the protein expression levels of Bax.

These results confirm that ISL can regulate the T24 cell cycle, specifically reduce the G2 phase sharply, and increase the accumulation of cells at the G1 phase, thereby inhibiting the growth and inducing apoptosis of BC T24 cells.

In conclusion, ISL can suppress the expression levels of PCNA and Bcl-2 *in vitro*, and up-regulate the expression of Bax, thus reducing the ratio of Bcl-2/Bax. This may be one of the molecular mechanisms of the ISL anti-tumor effect. The experimental results have great clinical significance for the treatment and cure of BC.

Conflict of interest

The authors declare no conflict of interest.

References

1. Bray F, Ferlay J, Soerjomataram I, Siegel RL, Torre LA, Jemal A. Global cancer statistics 2018: GLOBOCAN estimates of incidence and mortality worldwide for 36 cancers in 185 countries. CA Cancer J Clin 2018; 68: 394-424.
2. Das T, Sa G, Saha B, Das K. Multifocal signal modulation therapy of cancer: ancient weapon, modern targets. Mol Cell Biochem 2010; 336: 85-95.
3. Deng Q, Wang Z, Wang L, et al. Lower mRNA and protein expression levels of LC3 and Beclin1, markers of autophagy, were correlated with progression of renal clear cell carcinoma. Jpn J Clin Oncol 2013; 43: 1261-8.
4. Perez-Chacon G, Adrados M, Vallejo-Cremades MT, Lefebvre S, Reed JC, Zapata JM. Dysregulated TRAF3 and BCL2 expression promotes multiple classes of mature non-Hodgkin B cell lymphoma in mice. Front Immunol 2018; 9: 3114.
5. Tsujimoto Y, Shimizu S. Bcl-2 family: life-or-death switch. FEBS Lett 2000; 466: 6-10.
6. Qian YU, Qing-Ming LI, Wei-Kang WU, Zeng J. The reduced expression of PCNA and p53 protein in experimental rats stomach carcinoma by traditional Chinese Herb "WEI KANG NING". Acad J Sun Yat-Sen Univ Med Sci 2000.
7. Zhou Y, Ho WS. Combination of liquiritin, isoliquiritin and isoliquirigenin induce apoptotic cell death through upregulating p53 and p21 in the A549 non-small cell lung cancer cells. Oncol Rep 2014; 31: 298-304.
8. Wang KL, Hsia SM, Chan CJ, et al. Inhibitory effects of isoliquiritigenin on the migration and invasion of human breast cancer cells. Exp Opin Therap Targets 2013; 17: 337-49.
9. Kanazawa M, Satomi Y, Mizutani Y, et al. Isoliquiritigenin inhibits the growth of prostate cancer. Eur Urol 2003; 43: 580-6.
10. Hsu YL, Kuo PL, Chiang LC, Lin CC. Isoliquiritigenin inhibits the proliferation and induces the apoptosis of human non-small cell lung cancer a549 cells. Clin Exp Pharmacol Physiol 2004; 31: 414-8.
11. Zhang XR, Wang SY, Sun W, Wei C. Isoliquiritigenin inhibits proliferation and metastasis of MKN28 gastric cancer cells by suppressing the PI3K/AKT/mTOR signaling pathway. Mol Med Rep 2018; 18: 3429-36.
12. Zhang B, Lai Y, Li Y, et al. Antineoplastic activity of isoliquiritigenin, a chalcone compound, in androgen-independent human prostate cancer cells linked to G2/M cell cycle arrest and cell apoptosis. Eur J Pharmacol 2018; 821: 57-67.
13. Safdari Y, Khalili M, Ebrahimzadeh MA, Yazdani Y, Farajnia S. Natural inhibitors of PI3K/AKT signaling in breast cancer: emphasis on newly-discovered molecular mechanisms of action. Pharmacol Res 2015; 93: 1-10.
14. Wu CH, Chen HY, Wang CW, et al. Isoliquiritigenin induces apoptosis and autophagy and inhibits endometrial cancer growth in mice. Oncotarget 2016; 7: 73432-47.
15. Si L, Yang X, Yan X, Wang Y, Zheng Q. Isoliquiritigenin induces apoptosis of human bladder cancer T24 cells via a cyclin-dependent kinase-independent mechanism. Oncol Lett 2017; 14: 241-9.
16. Guo ZQ, Zhang DD, Pang L, Wang YT, Cao P, Zhang SL. Semen affects the biological behavior of HeLa cells by altering ERK signaling. Arch Med Sci 2020; 16: 915-23.
17. Guo H, He Y, Bu C, Peng Z. Antitumor and apoptotic effects of 5-methoxypsoralen in U87MG human glioma cells and its effect on cell cycle, autophagy and PI3K/Akt signaling pathway. Arch Med Sci 2019; 15: 1530-8.
18. Malich G, Markovic B, Winder C. The sensitivity and specificity of the MTS tetrazolium assay for detecting the in vitro cytotoxicity of 20 chemicals using human cell lines. Toxicology 1997; 124: 179-92.
19. Li Z, Guo D, Yin X, et al. Zinc oxide nanoparticles induce human multiple myeloma cell death via reactive oxygen species and Cyt-C/Apaf-1/Caspase-9/Caspase-3 signaling pathway in vitro. Biomed Pharmacother 2020; 122: 109712.
20. Ploeg M, Aben KK, Kiemeney LA. The present and future burden of urinary bladder cancer in the world. World J Urol 2009; 27: 289-93.
21. Zhao M, Wang K, Shang J, Liang Z, Zheng W, Gu J. MiR-345-5p inhibits tumorigenesis of papillary thyroid carcinoma by targeting SETD7. Arch Med Sci 2020; 16: 888-97.
22. Eken MK, Ersoy GS, Kaygusuz EI, et al. Etanercept protects ovarian reserve against ischemia/reperfusion injury in a rat model. Arch Med Sci 2019; 15: 1104-12.
23. Zhou GS, Song LJ, Yang B. Isoliquiritigenin inhibits proliferation and induces apoptosis of U87 human glioma cells in vitro. Mol Med Rep 2013; 7: 531-6.

24. Wang TT, Chen ZZ, Xie P, et al. Isoliquiritigenin suppresses the proliferation and induced apoptosis via miR-32/LATS2/Wnt in nasopharyngeal carcinoma. Eur J Pharmacol 2019; 856: 172352.
25. Tian T, Sun J, Wang J, Liu Y, Liu H. Isoliquiritigenin inhibits cell proliferation and migration through the PI3K/AKT signaling pathway in A549 lung cancer cells. Oncol Lett 2018; 16: 6133-9.
26. Chen J, Liu C, Yang QQ, et al. Isoliquiritigenin suppresses osteosarcoma U2OS cell proliferation and invasion by regulating the PI3K/Akt signalling pathway. Chemotherapy 2018; 63: 155-61.
27. Kirkin V, Joos S, Zörnig M. The role of Bcl-2 family members in tumorigenesis. Biochim Biophys Acta 2004; 1644: 229-49.
28. Hsu YL, Chia CC, Chen PJ, Huang SE, Huang SC, Kuo PL. Shallot and licorice constituent isoliquiritigenin arrests cell cycle progression and induces apoptosis through the induction of ATM/p53 and initiation of the mitochondrial system in human cervical carcinoma HeLa cells. Mol Nutr Food Res 2009; 53: 826-35.
29. Chen L, Li Q, Wang J, et al. MiR-29b-3p promotes chondrocyte apoptosis and facilitates the occurrence and development of osteoarthritis by targeting PGRN. J Cell Mol Med Rep 2017; 21: 3347-59.